MAX-PLANCK-INSTITUT
FÜR PLASMAPHYSIK

Gyrokinetic pedestal shaping studies (& ion frequency ETG)

ASDEX Upgrade

TSVV1 workshop 2025

F Sheffield, T Görler, L Radovanovic, E Wolfrum, G Merlo, C Angioni, F Jenko and the ASDEX Upgrade team

Structure of this presentation

- Introduction, experimental scenario & main goals
- Linear characterization of microinstabilities
- A (short) dive into ion frequency ETGs
- Nonlinear ion scale turbulence simulations
- Nonlinear electron scale turbulence simulations
- Comparisons with experimental fluxes
- Summary and Outlook

The GENE code

[F. Jenko et al, PoP (2000)]
[T. Görler et al, JCP (2011)]

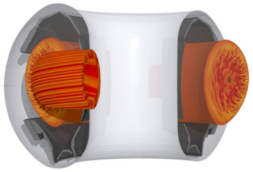

[genecode.org]

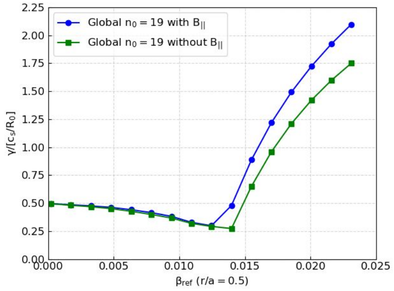

Global linear

Global nonlinear

Local linear

Local nonlinear

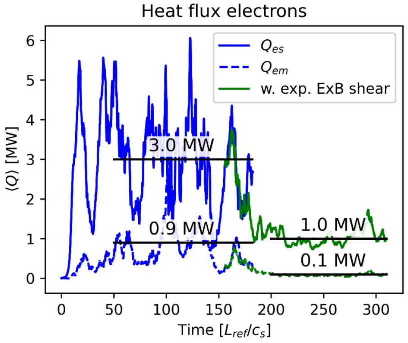

[L. A. Leppin, PhD thesis (2024)]

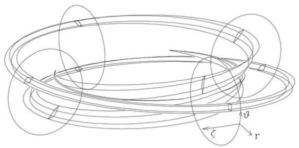

[M. A. Beer, PhD thesis (1995)]

Experimental scenario: ELMy H-mode

Low shaping δ_{up}=0.10, κ=1.6

While fixing β_{pol}

High shaping δ_{up}=0.25, κ=1.7

discharge #	β_{pol}	β_N	I_P	B_T	NBI	ICRH	ECRH	q_{95}
#38472	1.35	1.95	800kA	-2.5T	4-10MW	2MW	/	5.1-5.6

[L. Radovanovic et al., NF (2025)]

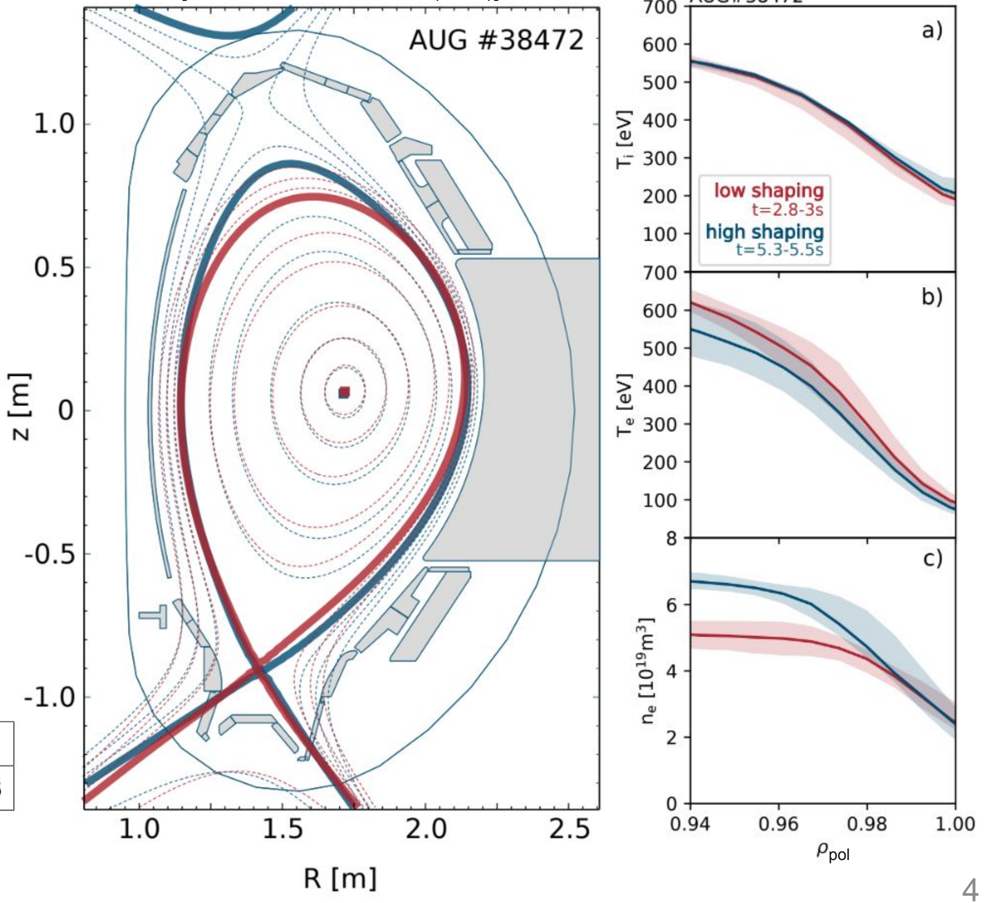

Pedestal shaping studies

Main Goals

- Characterize the pedestal microinstabilities on both high and low shaping
- How does stabilization from different sources in the pedestal change based on shaping?
- How does anomalous transport in the pedestal change when we change the shaping?

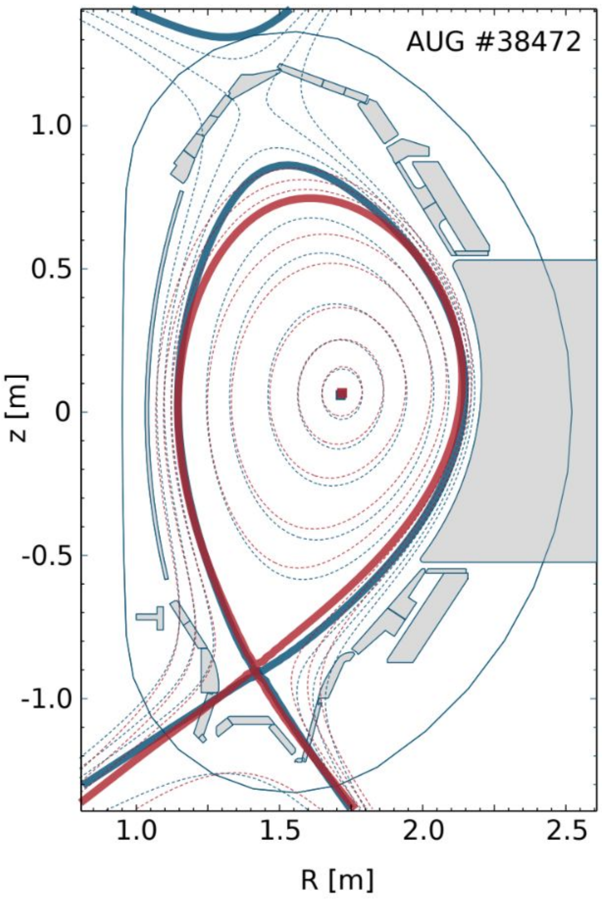

Local linear characterization

- Local simulations as initial approach
- Easy to select specific modes and characterize dominant microinstabilities
- Refinement of previous scans*
- Unclear how well these would match up with higher fidelity approaches

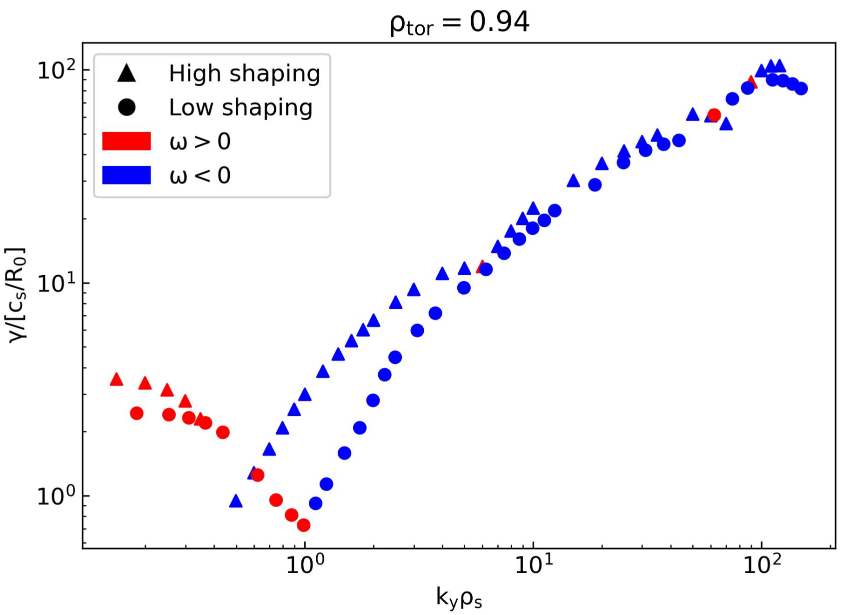

Growth rate maximized over ballooning angle

ϕxn cross phase ~ 0.7 for ion scale modes

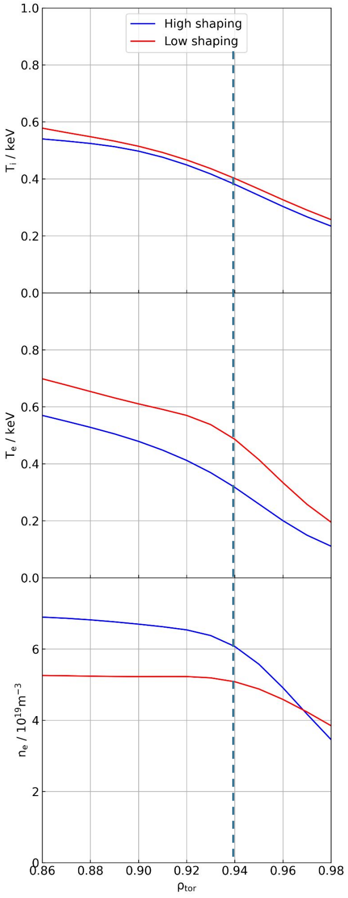

*Initial scans performed in [L. Radovanovic et al., PhD thesis (2025)]

Local linear characterization

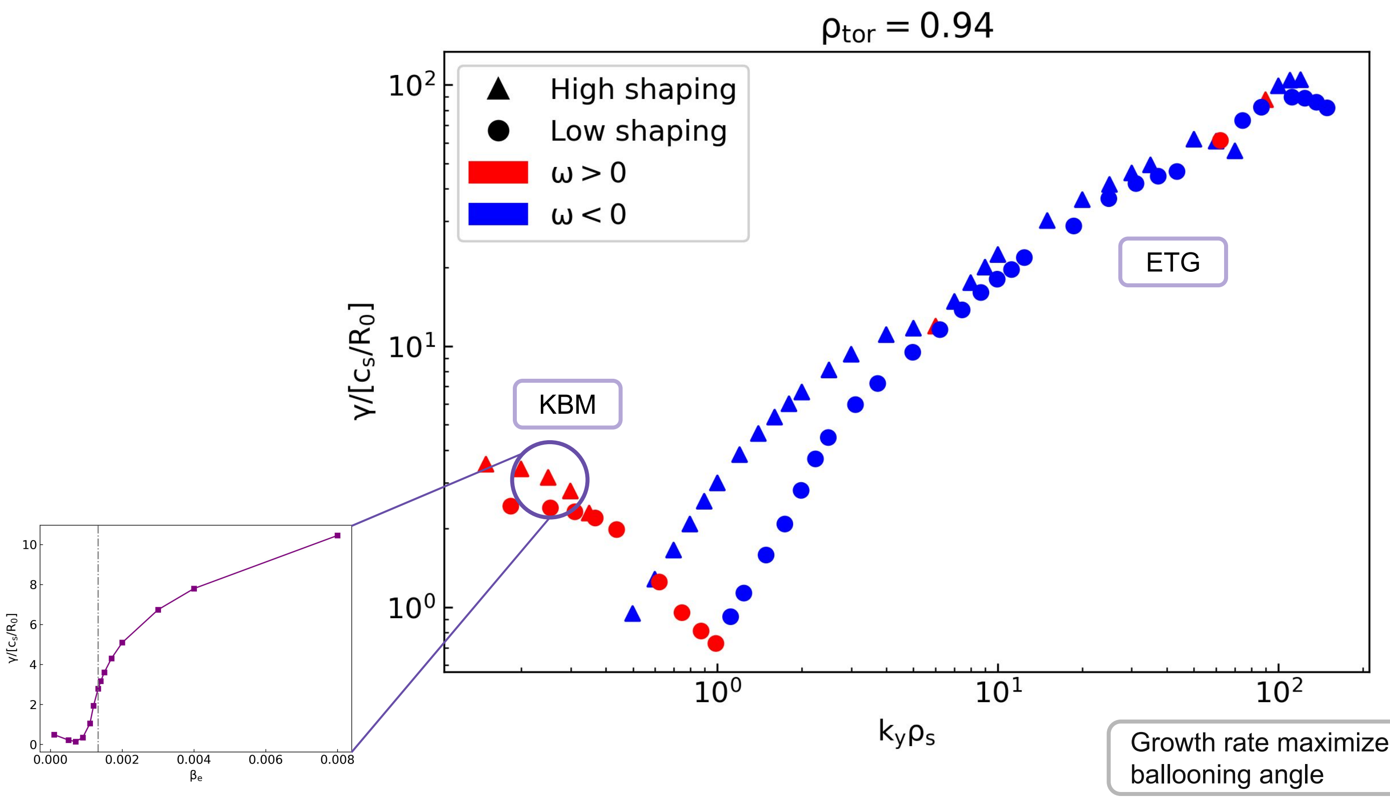

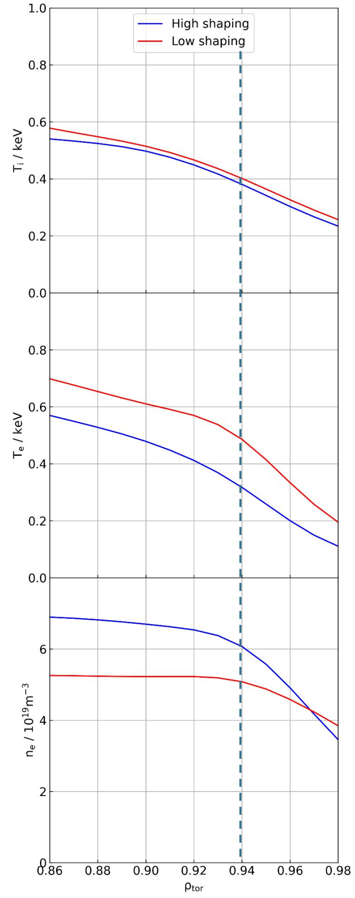

Growth rate maximized over ballooning angle

ϕxn cross phase ~ 0.7 for ion scale modes

Grid size: $(n_s, n_x, n_z, n_v, n_w) = (2, 15, 64, 48, 16)$; Physics: D/e species, EM, collisions, no ExB shear, no impurities

Local linear characterization

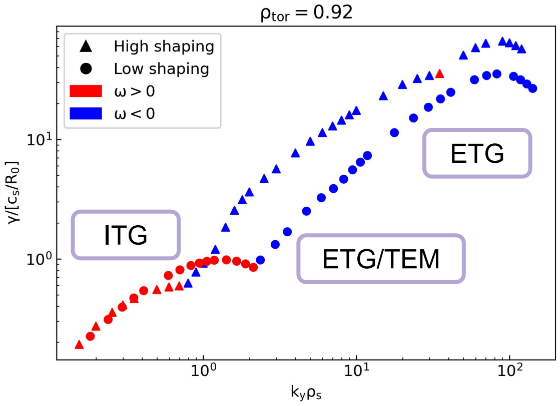

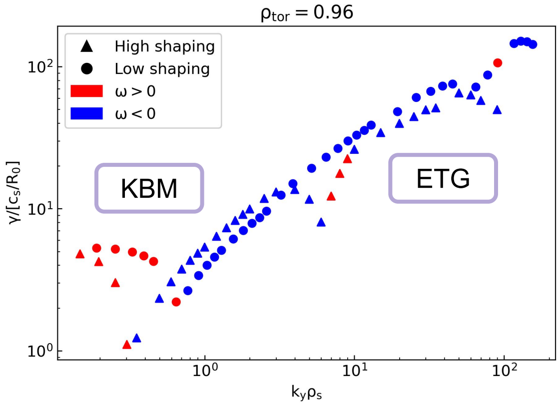

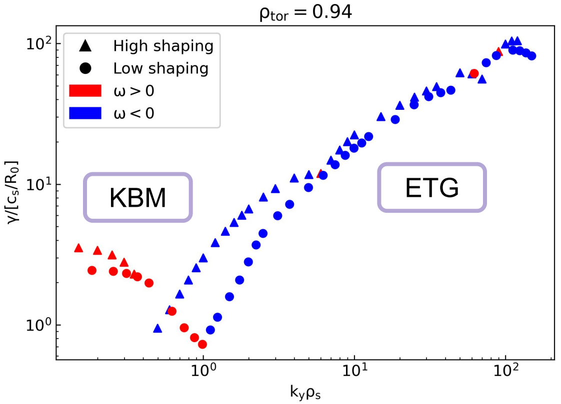

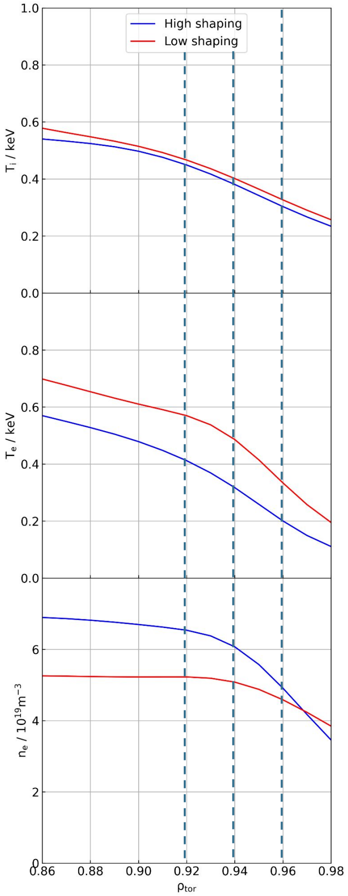

Growth rate maximized over ballooning angle

ϕxn cross phase ~ 0.7 for ion scale modes

Grid size: $(n_s,n_x,n_z,n_v,n_w)=(2,15,64,48,16)$; Physics: D/e species, EM, collisions, no ExB shear, no impurities

Local linear characterization

Positive frequencies on electron scales

Is that physical?

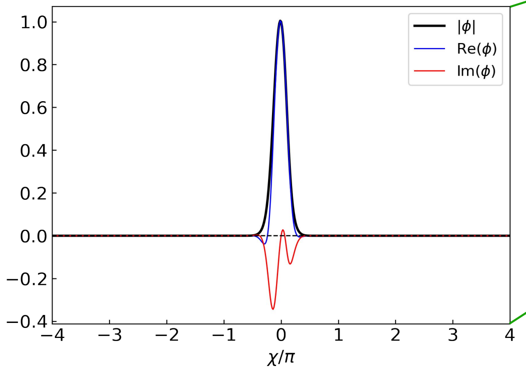

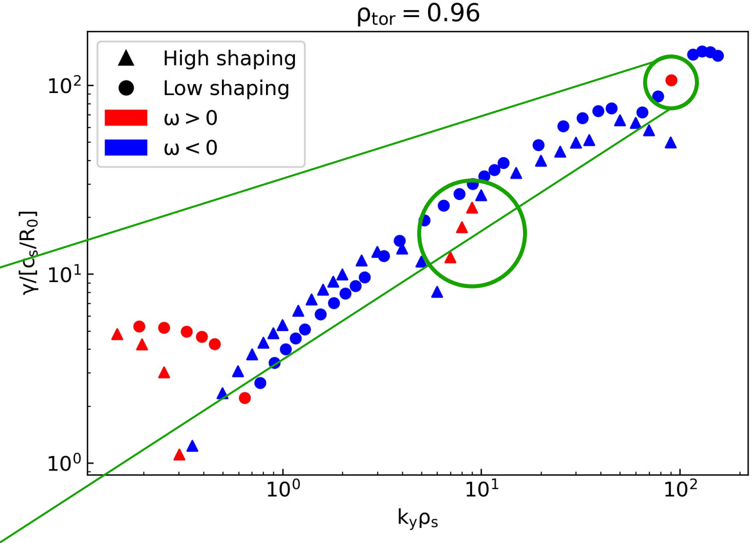

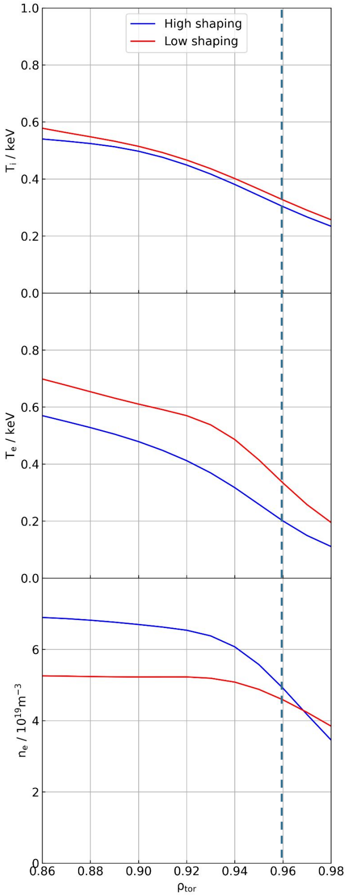

On ion frequency ETG

We do have precedence on linear and nonlinear pedestal GENE simulations

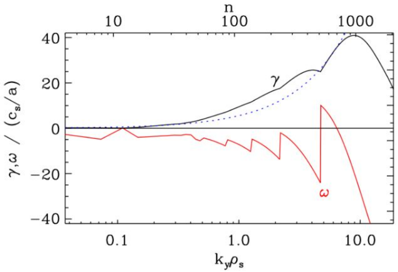

Figure 2. Growth rate (black) and frequency (red) spectra across all scales. The first two points ($n = 4, 8$) are MT, the remainder various ETG branches. A dotted blue line indicates linear scaling $\gamma \propto k_y$.

[M.J. Pueschel et al, NF (2020)]

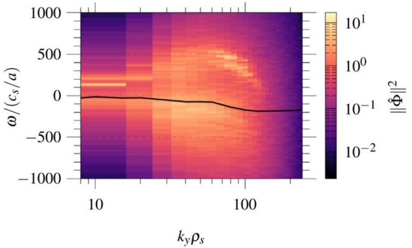

FIG. 8. The spectrum of $\hat{\Phi}$ at $k_x = 0$ is plotted as a function of k_y and ω, along with a black line indicating the frequencies $\omega(k_y)$ of the most unstable linear modes. Data are from case 5.

[J. Walker & D. Hatch, PoP (2023)]

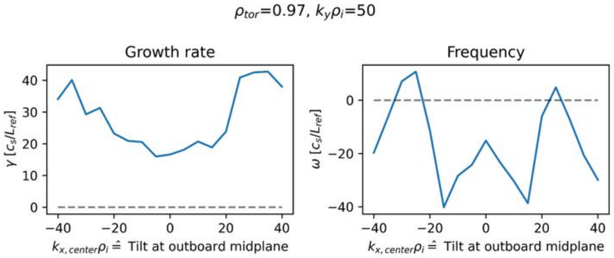

[L. Leppin, PhD thesis (2023)]

On ion frequency ETG

[F. Sheffield et al, submitted to PoP (2025)]

- Run and compare GENE simulations with an ETG dispersion relation [J. F. Parisi et al, NF (2020)]
- Can we find these ETG modes (semi) analytically?
- When do these modes appear? Why at the pedestal?

On ion frequency ETG

[F. Sheffield et al, submitted to PoP (2025)]

- Run and compare GENE simulations with an ETG dispersion relation [J. F. Parisi et al, NF (2020)]
- Can we find these ETG modes (semi) analytically?
- When do these modes appear? Why at the pedestal?

High $k_y \varrho_s$ (~70)

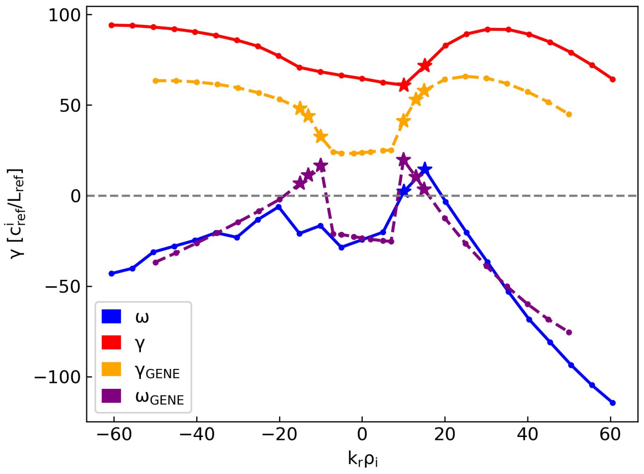

Low $k_y \varrho_s$ (~8)

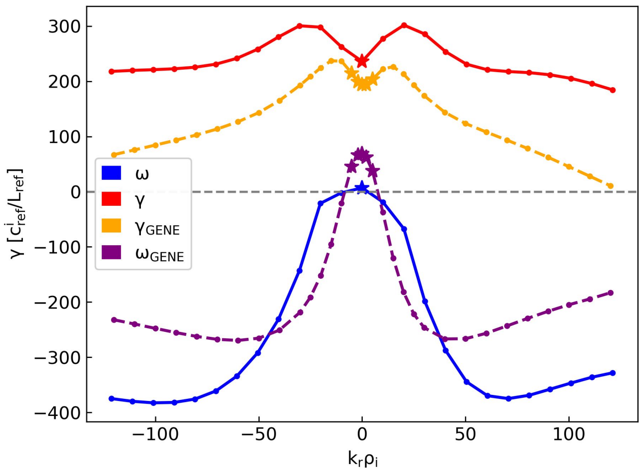

On ion frequency ETG

[F. Sheffield et al, submitted to PoP (2025)]

Quick summary of what we found:

- Ion frequency ETG can be seen analytically and transition smoothly to these frequencies.
- Pedestal physics favour their formation via large gradients, safety factor, drift frequencies and geometry.
- On core plasmas, the ETG η threshold prevents their formation.

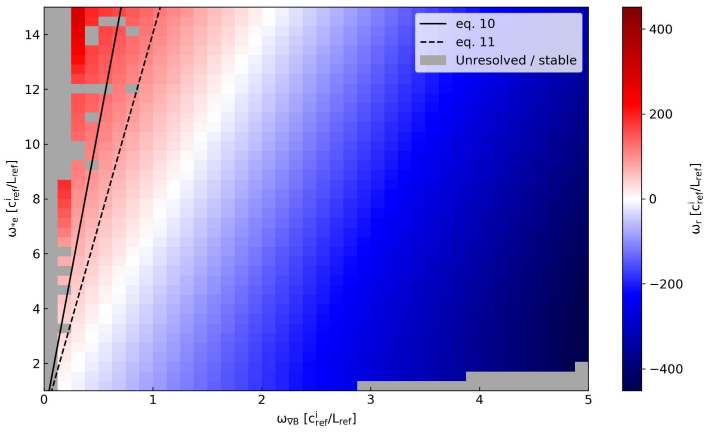

Back to shaping studies

Global ion scale turbulence

Will we see the same behaviour with higher fidelity?

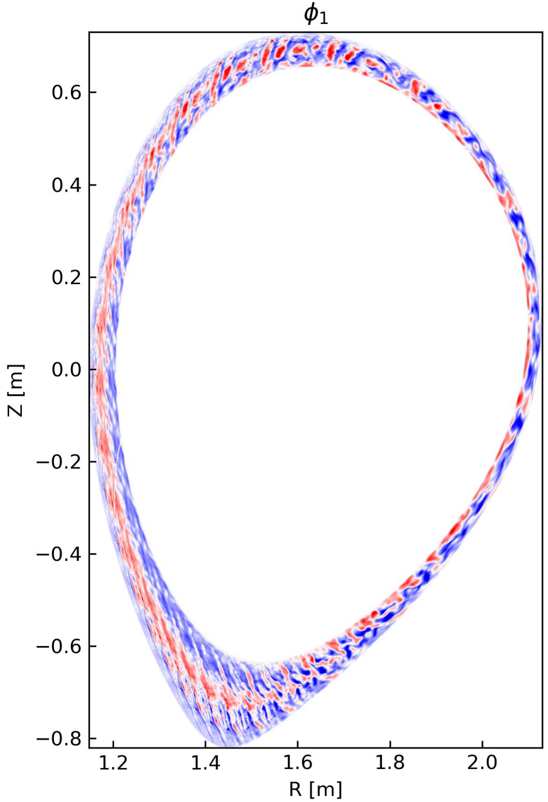

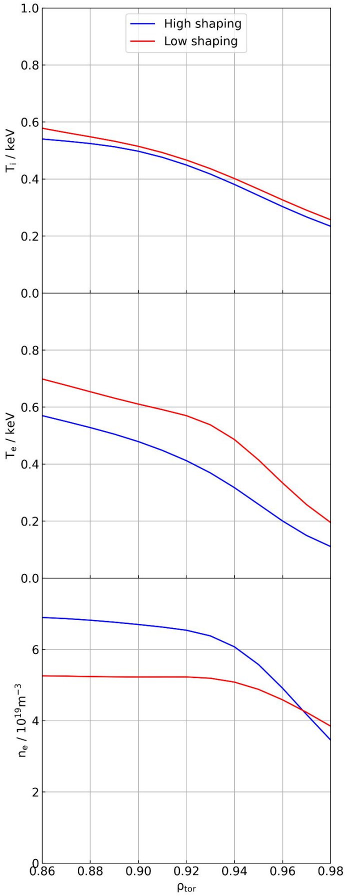

Grid size: (n_s,n_x,n_{ky},n_z,n_v,n_w)=(2,256/512,32,64,64,32); Physics: D/e species, EM, collisions, impurities, ExB shear

Global ion scale turbulence

w/ ExB shear
w/ impurities

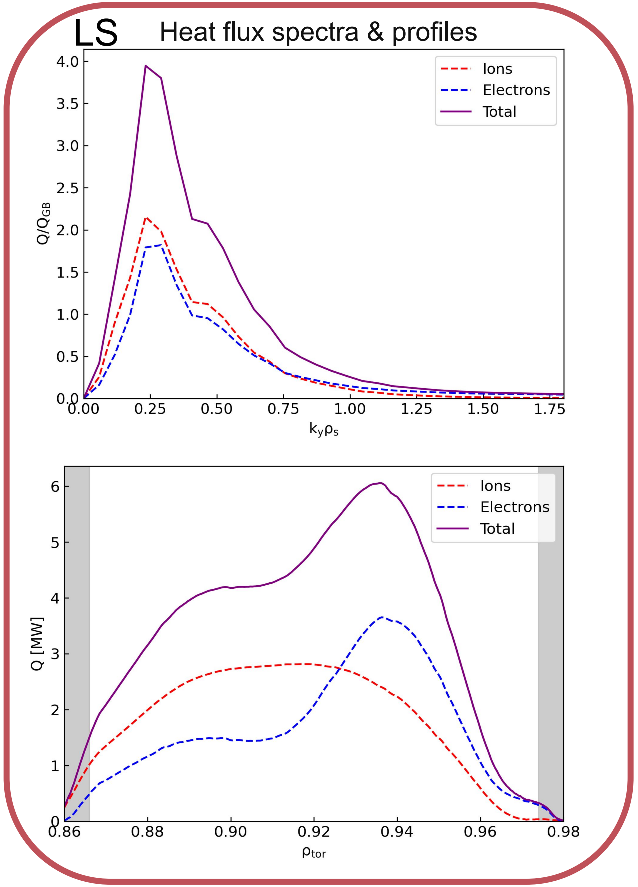

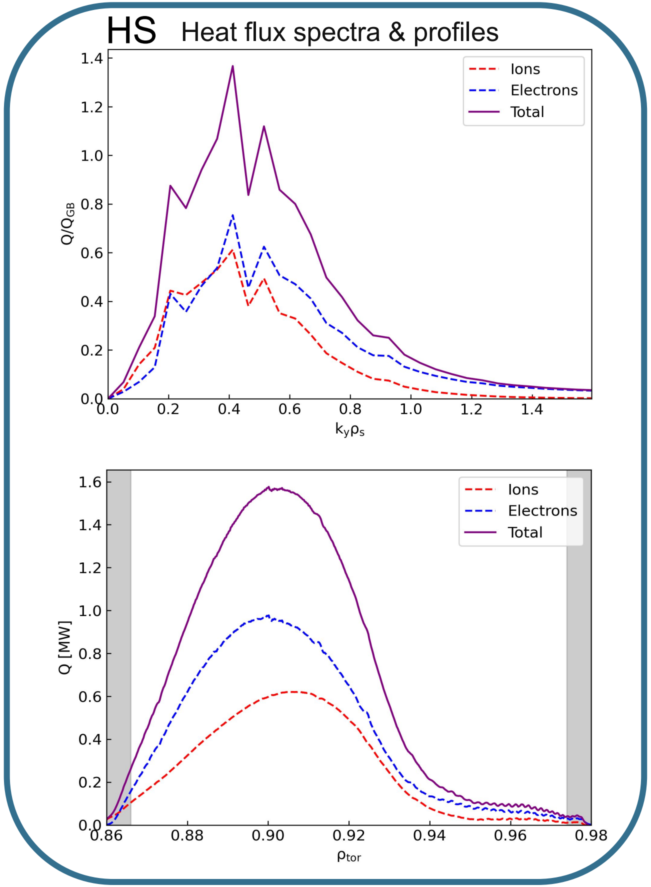

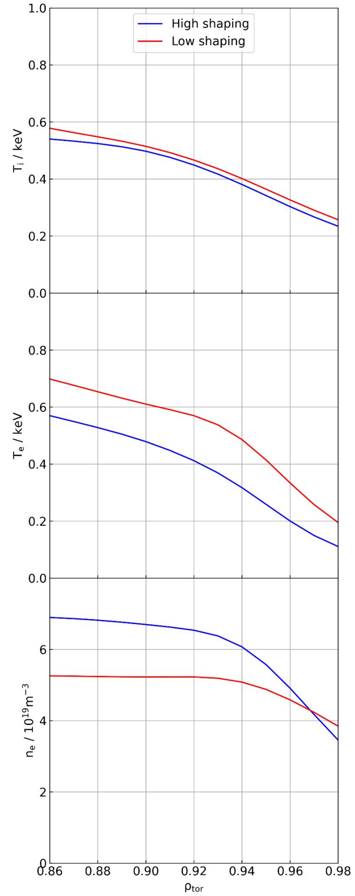

Global ion scale turbulence

w/ ExB shear
w/ impurities

LS

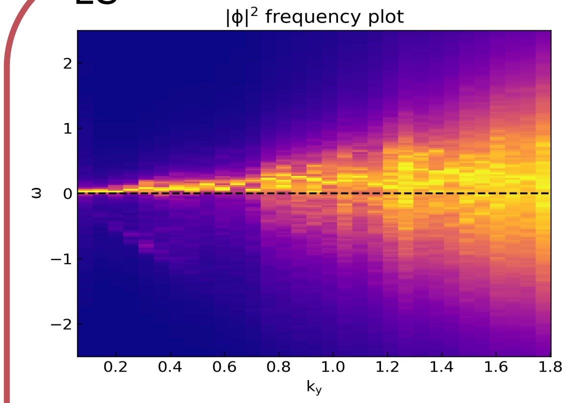

ITG or KBM.. but low frequency?

HS

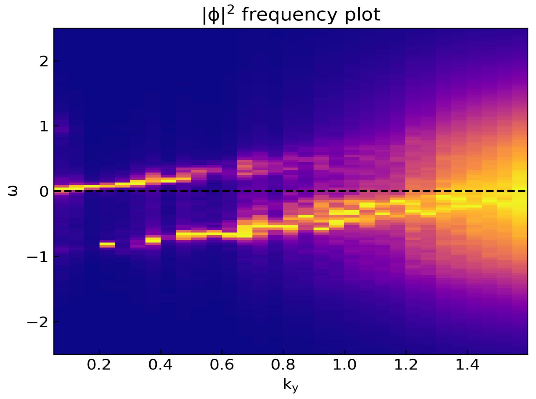

Possibly ITG/TEM turbulence

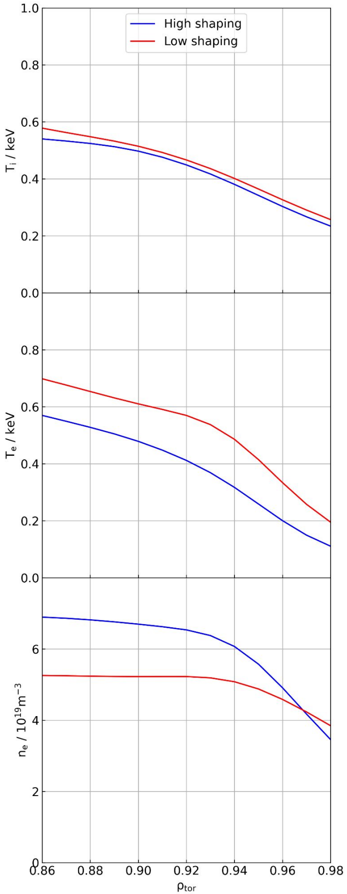

Global ion scale turbulence

w/ ExB shear
w/ impurities

LS

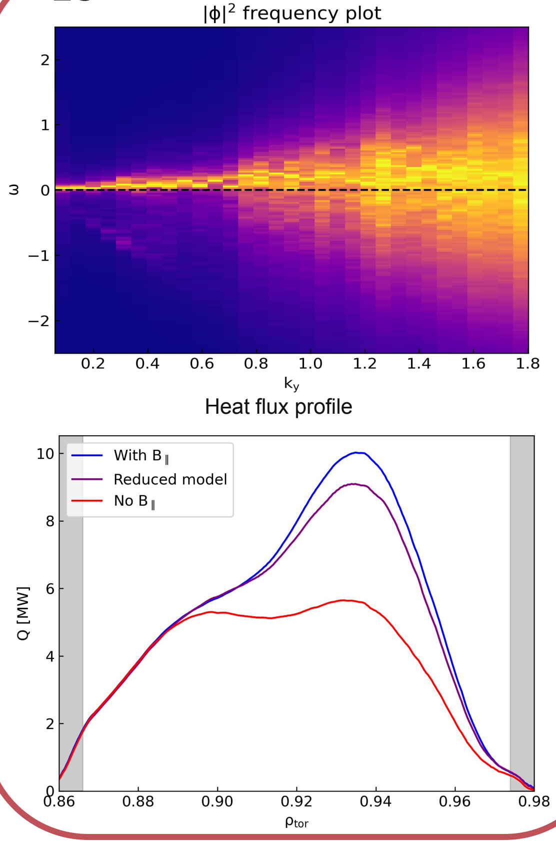

HS

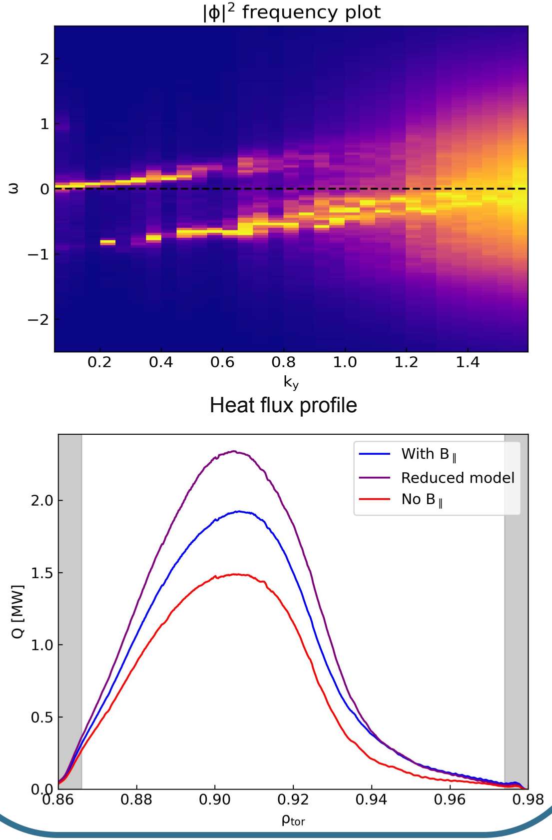

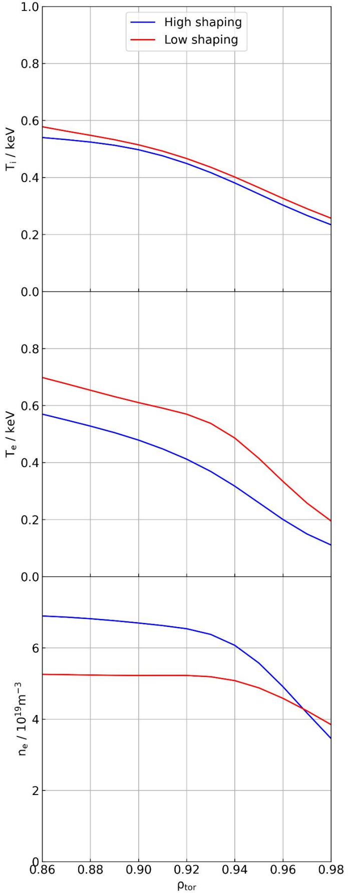

Fully electromagnetic! [F. Sheffield et al., PPCF (2025)]

Global ion scale turbulence

w/ ExB shear
w/ impurities

Much higher particle flux in LS

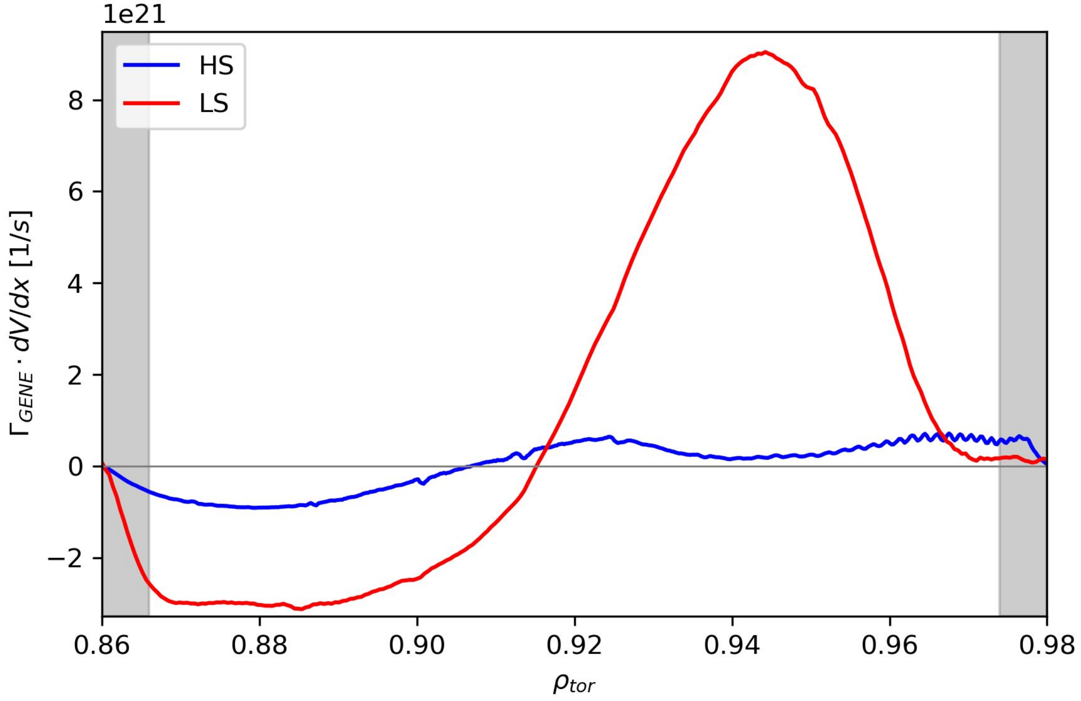

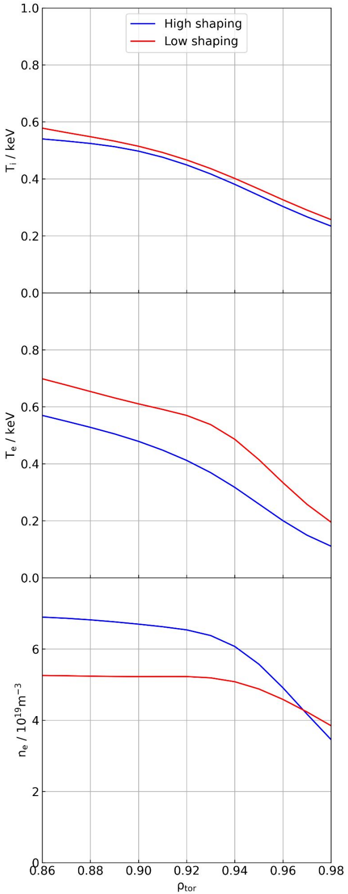

Overview of the case from the gyrokinetic perspective

Low shaping equilibrium with KBM-hybrid activity

Increase in shaping keeping β_{pol} constant

Stabilization of KBM-hybrid

Dominant ITG/TEM turbulence

Since the dominant mode no longer drives particle flux, the density increases

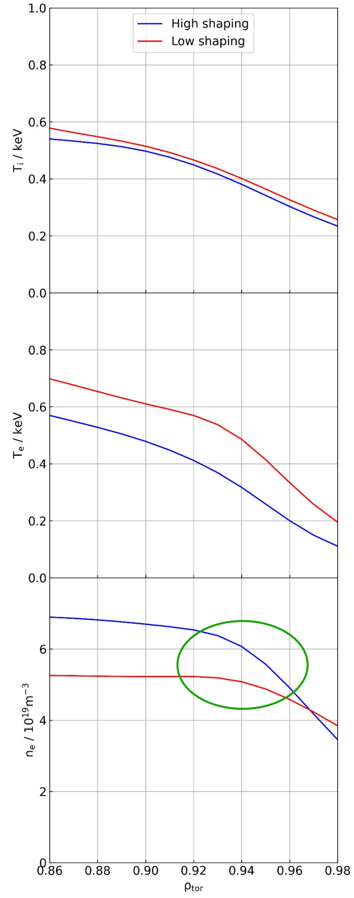

Global ion scale turbulence

- Main modes encountered locally appear in our global nonlinear simulations

- Change in behaviour from low shaping to high shaping suggesting hybrid-KBM for LS and ITG/TEM for HS

- Hybrid-KBM activity at LS could explain the increase in density for HS

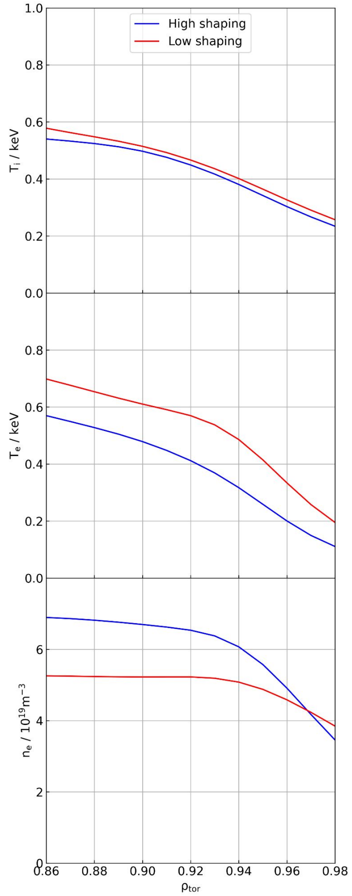

Global ion scale turbulence

- Main modes encountered locally appear in our global nonlinear simulations

- Change in behaviour from low shaping to high shaping suggesting hybrid-KBM for LS and ITG/TEM for HS

- Hybrid-KBM activity at LS could explain the increase in density for HS

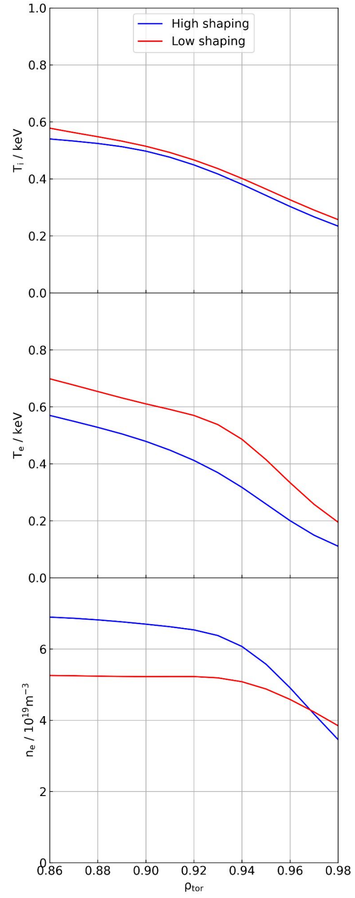

And what about electron scales?

Local electron scale turbulence

- Small scales are naturally more localized
- High parallel resolution is needed
- Different branches of ETG can appear (toroidal, slab)
- Quite useful to compare with reduced models for ETG

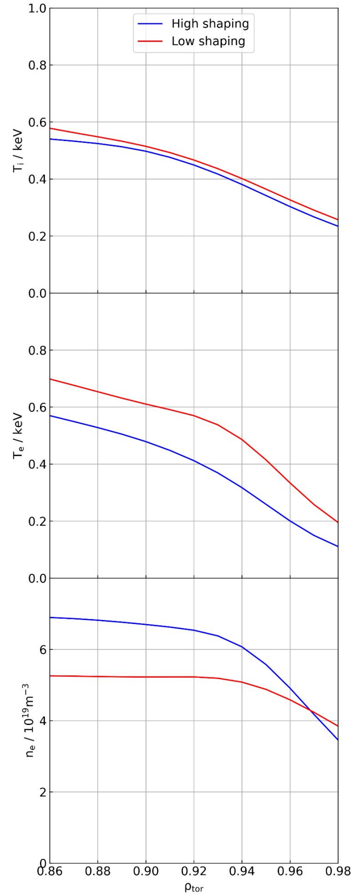

Local electron scale turbulence

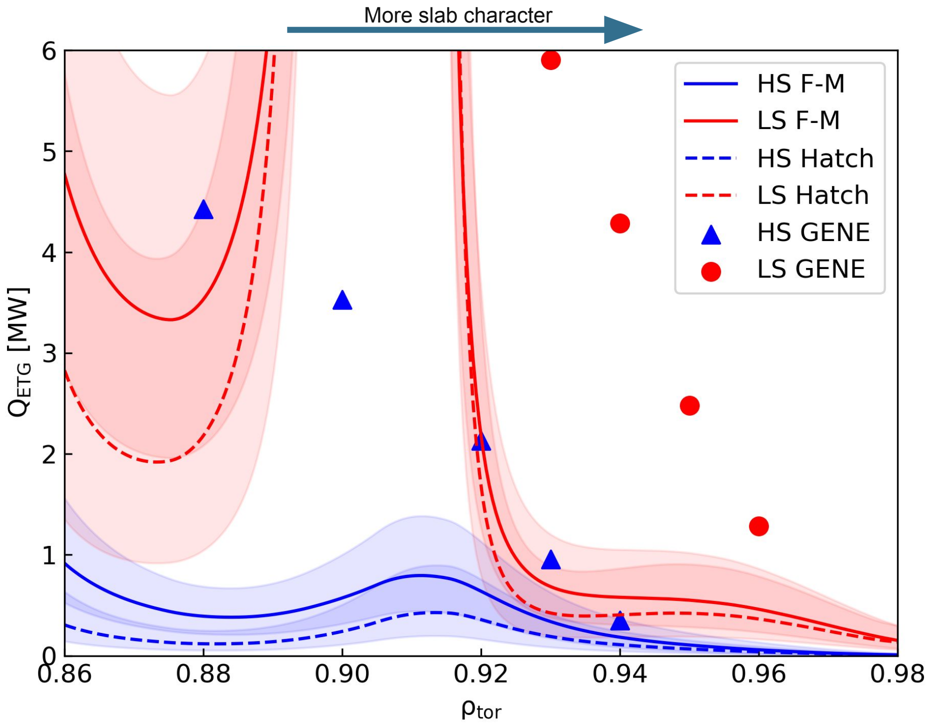

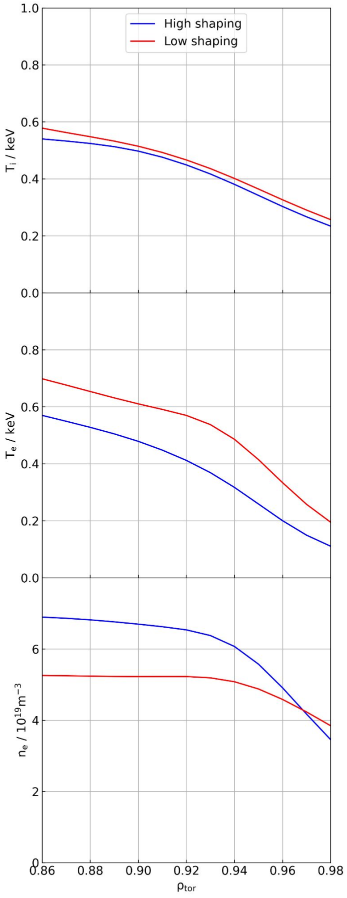

[D.R. Hatch et al, NF (2024)]
[Farcaş I-G, Merlo G, Jenko F, JPP (2024)]

Grid size: $(n_s,n_x,n_{ky},n_z,n_v,n_w)=(1,256+,48,512,32,16)$; Physics: e species, collisions, no ExB shear

Local electron scale turbulence

- HS has consistently less ETG transport than LS across the pedestal.
- Reduced models recover general trends, but refinements are necessary.

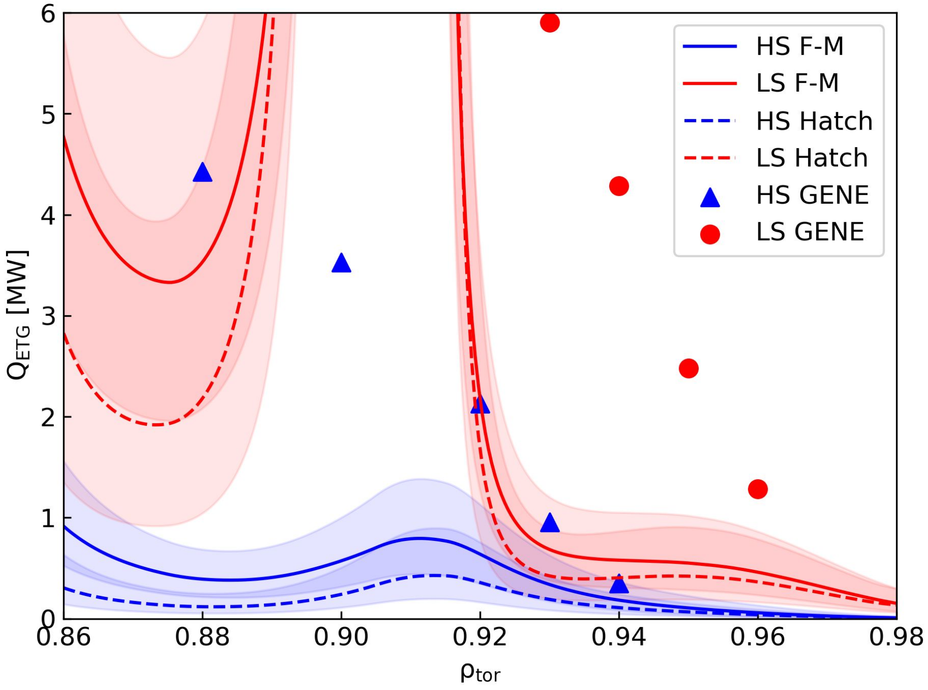

[D.R. Hatch et al, NF (2024)]
[Farcaş I-G, Merlo G, Jenko F, JPP (2024)]

Grid size: $(n_s,n_x,n_{ky},n_z,n_v,n_w)$=(1,256+,48,512,32,16); Physics: e species, collisions, no ExB shear

Comparisons with experimental fluxes

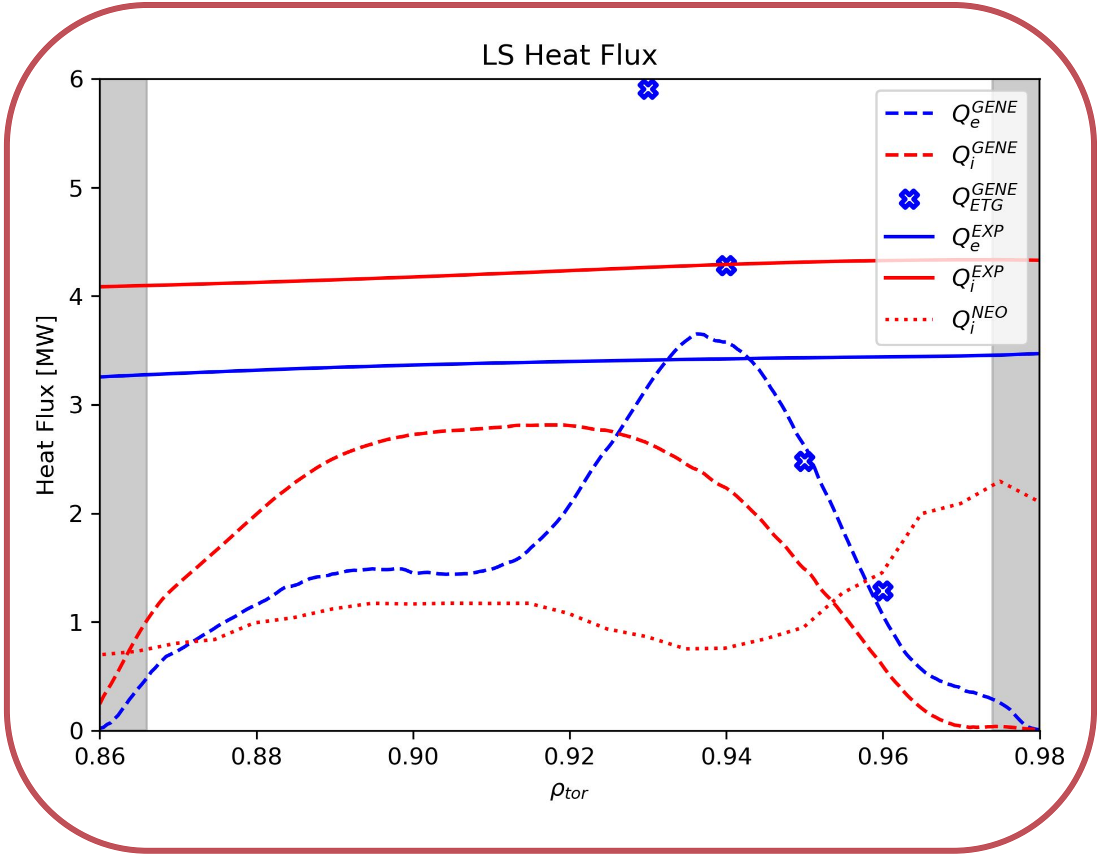

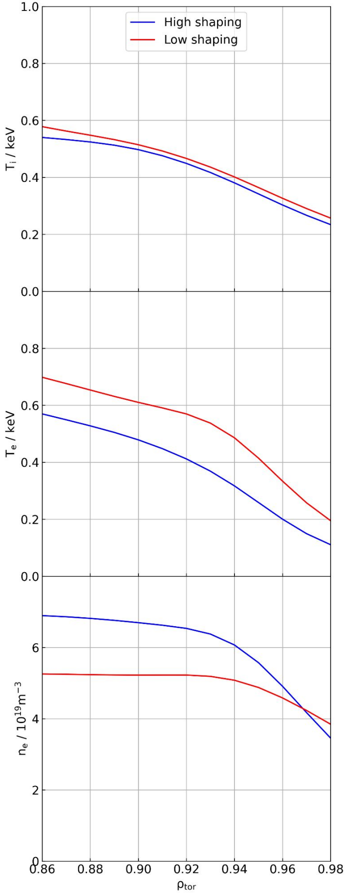

Comparisons with experimental fluxes

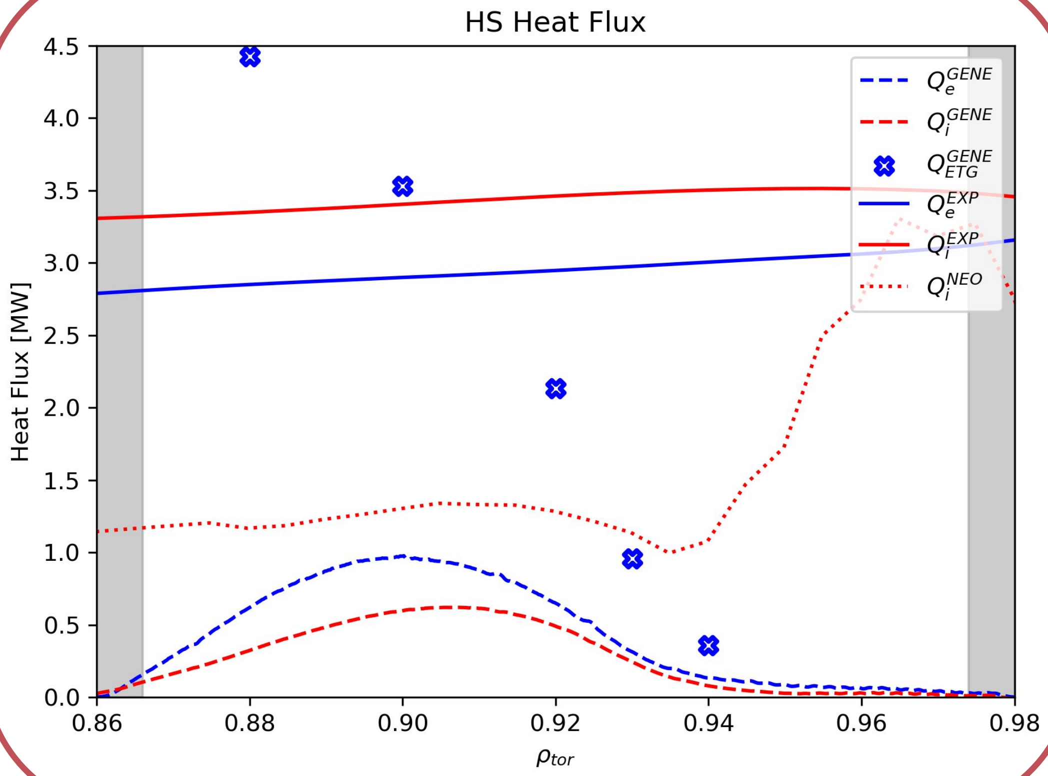

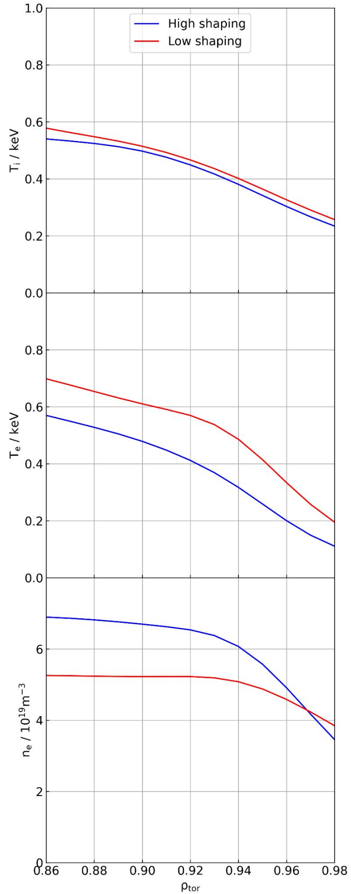

Summary and Outlook

- ★ Dominant modes in local linear simulations are present in the global nonlinear ones.
- ★ ETG modes can propagate in the ion diamagnetic direction in the pedestal.
- ★ At ion scales LS seems dominated by a KBM-hybrid while HS seems ITG/TEM dominated.
- ★ The change in shaping induces a stabilization of the KBM-hybrid, which in turn decreases the particle transport and increases the plasma density.
- ★ Local ETG simulations have lower transport for HS, with reduced models recovering general trends but underestimating transport.
- ★ Comparisons with experiment show qualitative agreement at ion scale for LS and an underestimation of transport for HS (possibly due to measurement uncertainties and/or multiscale interactions)

- ➢ Further studies on the KBM-hybrid and additional ETG simulations are ongoing.

Summary and Outlook

- ★ Dominant modes in local linear simulations are present in the global nonlinear ones.
- ★ ETG modes can propagate in the ion diamagnetic direction in the pedestal.
- ★ At ion scales LS seems dominated by a KBM-hybrid while HS seems ITG/TEM dominated.
- ★ The change in shaping induces a stabilization of the KBM-hybrid, which in turn decreases the particle transport and increases the plasma density.
- ★ Local ETG simulations have lower transport for HS, with reduced models recovering general trends but underestimating transport.
- ★ Comparisons with experiment show qualitative agreement at ion scale for LS and an underestimation of transport for HS (possibly due to measurement uncertainties and/or multiscale interactions)

- ➢ Further studies on the KBM-hybrid and additional ETG simulations are ongoing.

Thank you

Backup slides: linear characterization

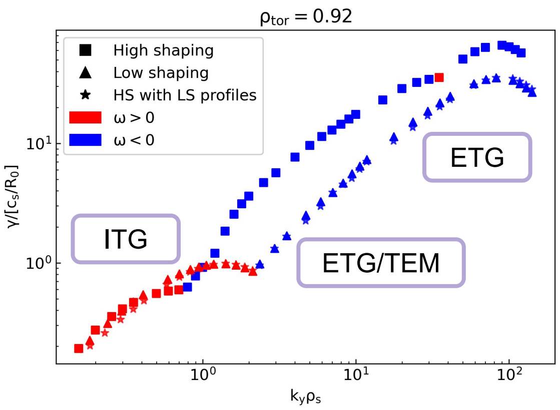

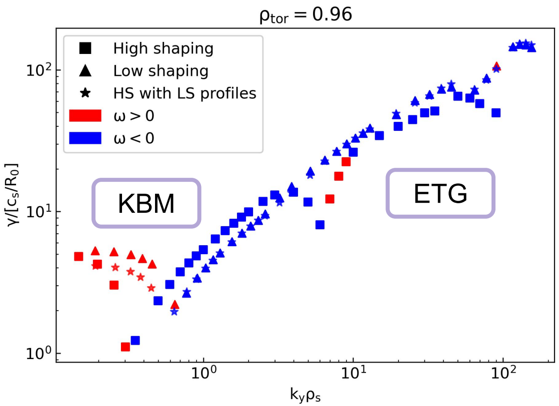

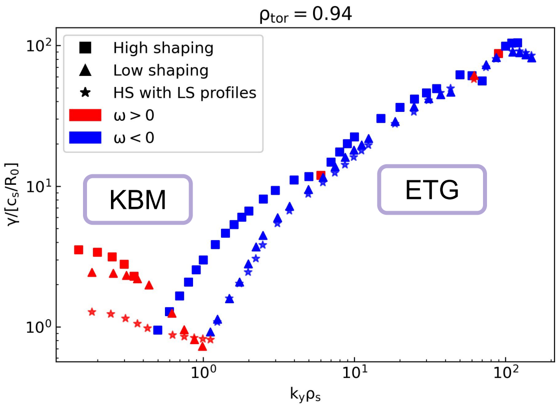

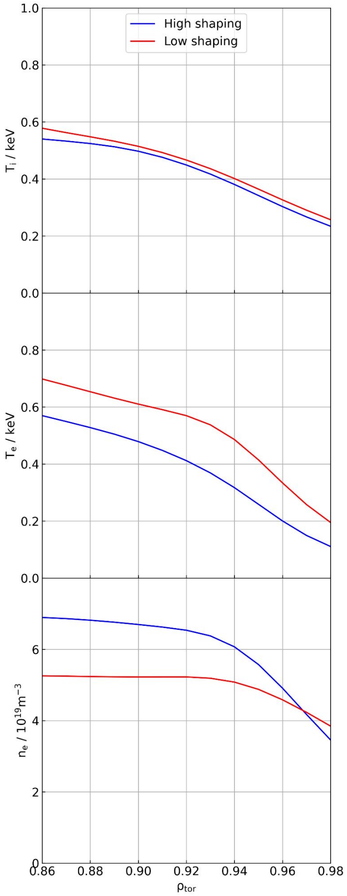

Growth rate maximized over ballooning angle

ϕxn cross phase ~ 0.7 for ion scale modes

Global ion scale turbulence - effect of ExB shear and impurities

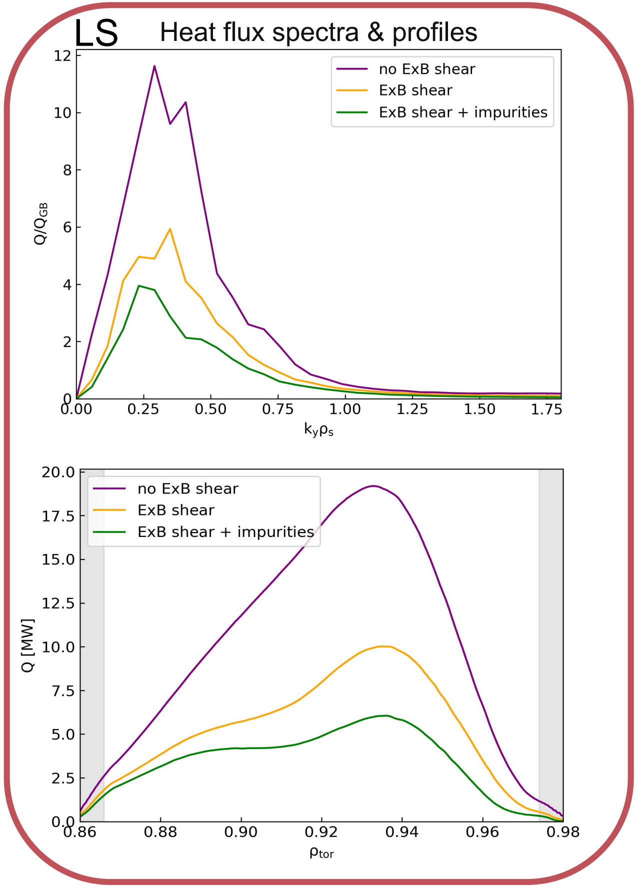

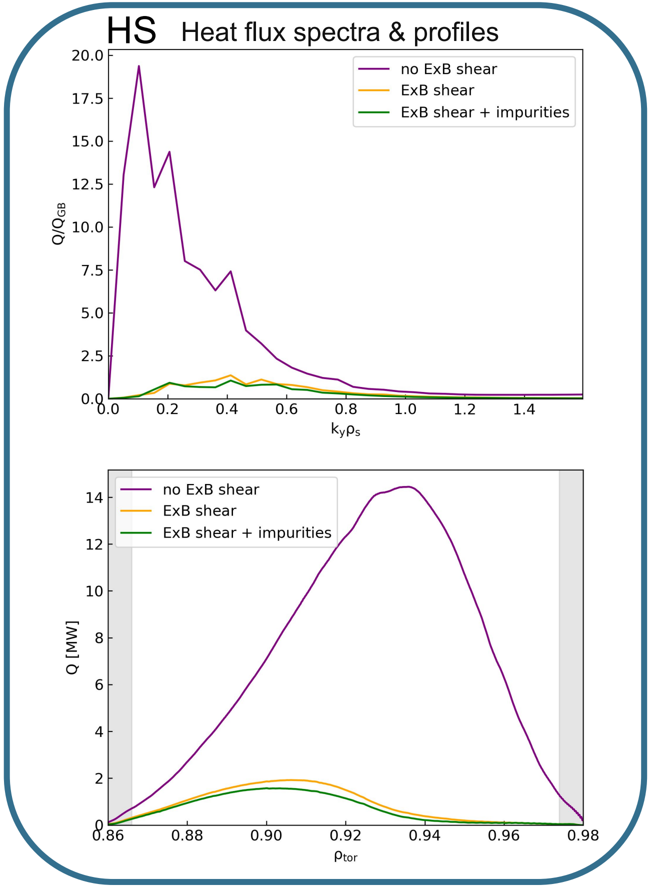

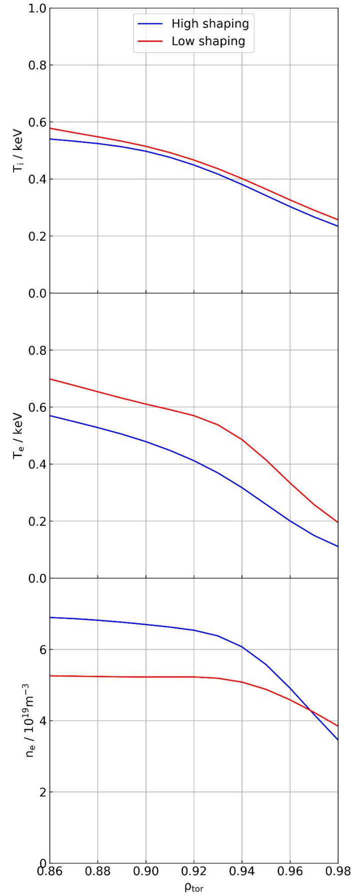

Global ion scale turbulence - no shear or impurities

No ExB shear
No impurities

LS Heat flux spectra & profiles

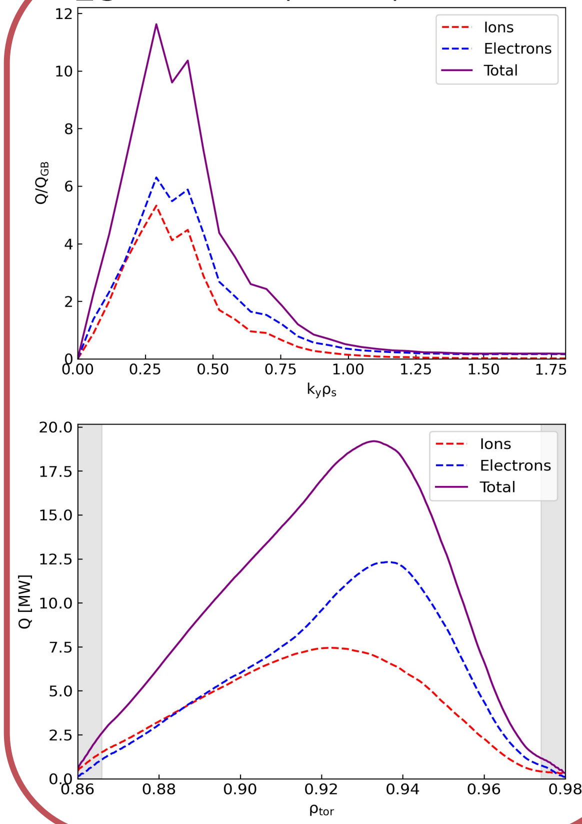

HS Heat flux spectra & profiles

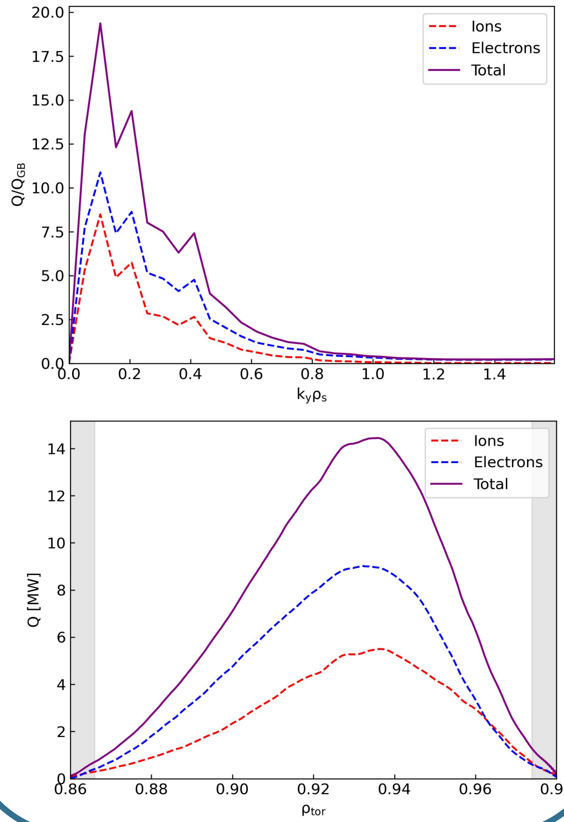

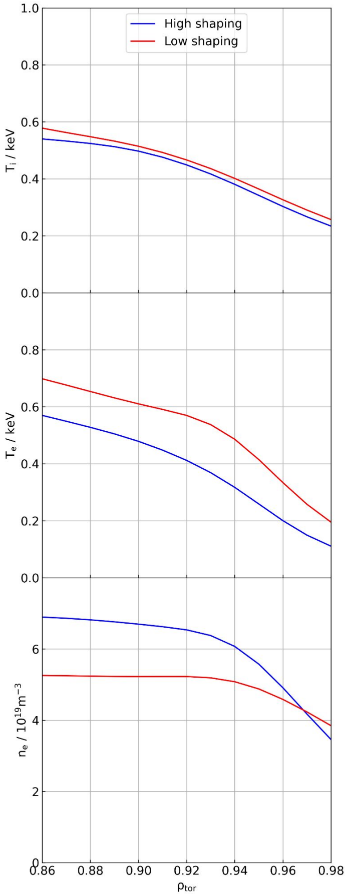

Backup slides - Er and beta crit

Er of the discharge

$$\beta_{\mathrm{crit}}^{\mathrm{MHD}} = \frac{0.6\hat{s}}{q_0^2(2\omega_n + \omega_{T\mathrm{i}} + \omega_{T\mathrm{e}})}$$

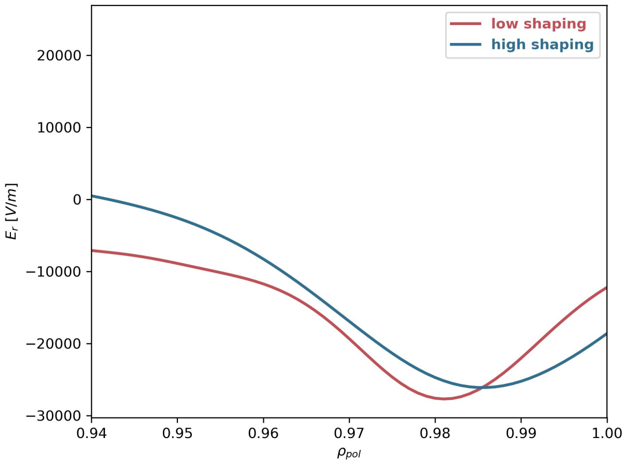

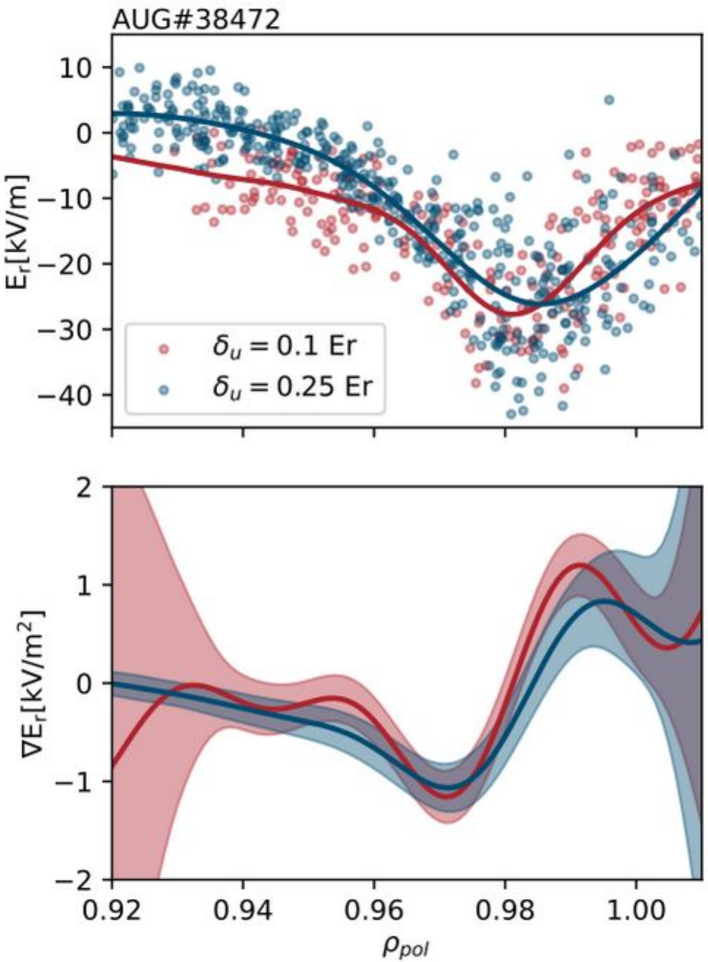

Backup slides - Qgb related figures

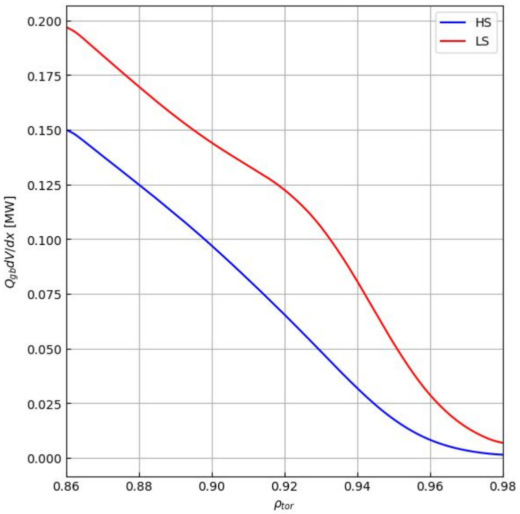

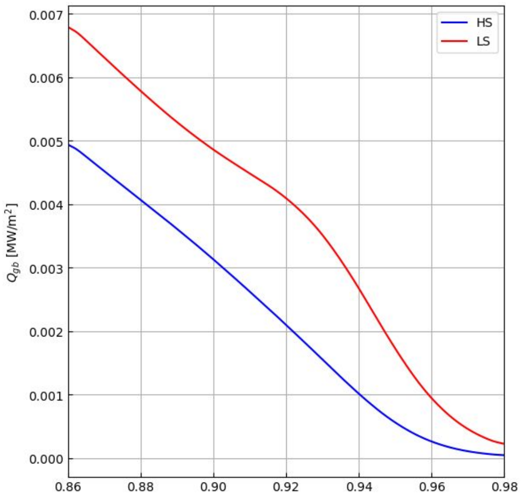

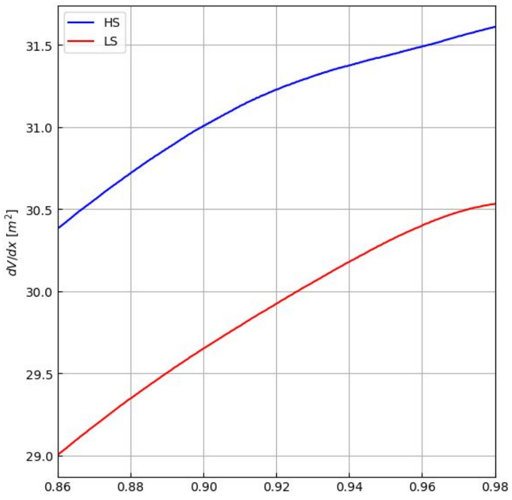

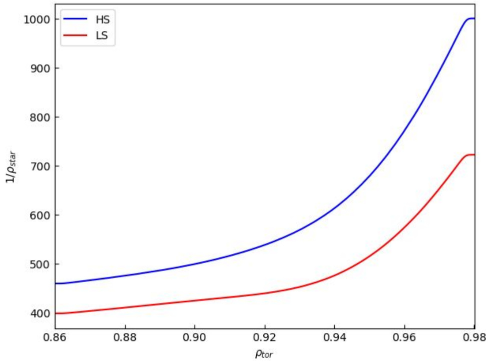

Backup slides - Beta scans

x0=0.96

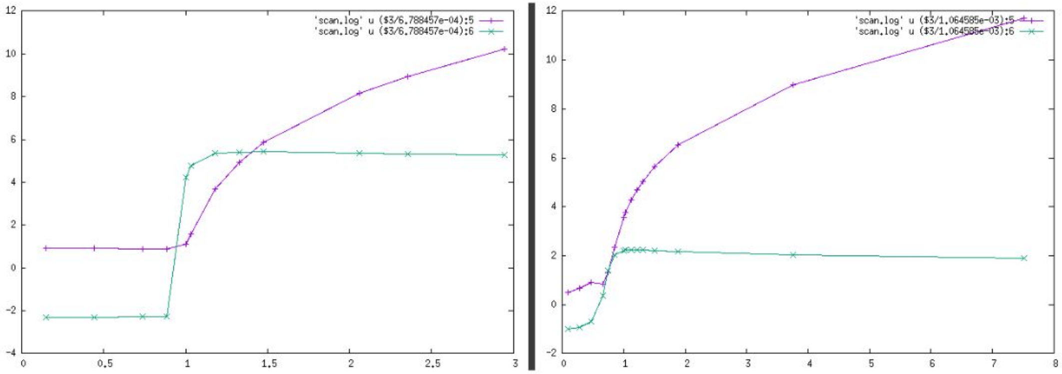

Figure 3: β scan of HS (left) and LS (right). Growth rate and frequency are shown. β values are normalized to the respective nominal value.

x0=0.92

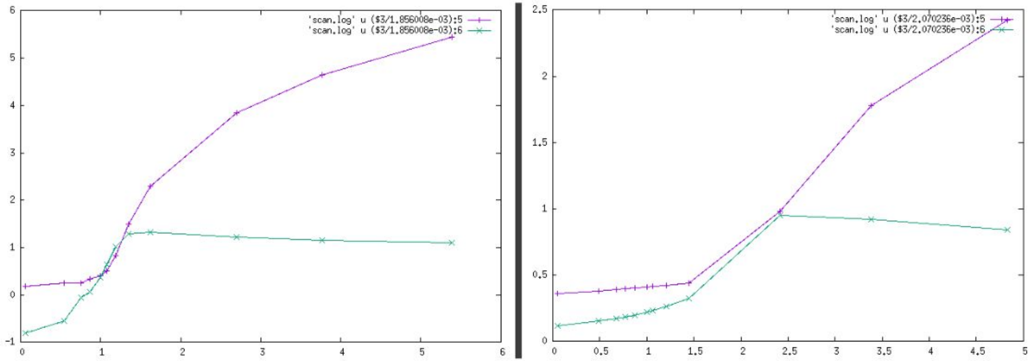

Figure 5: Standard beta scan. HS on the left and LS on the right.

Backup slides - ion frequency ETG

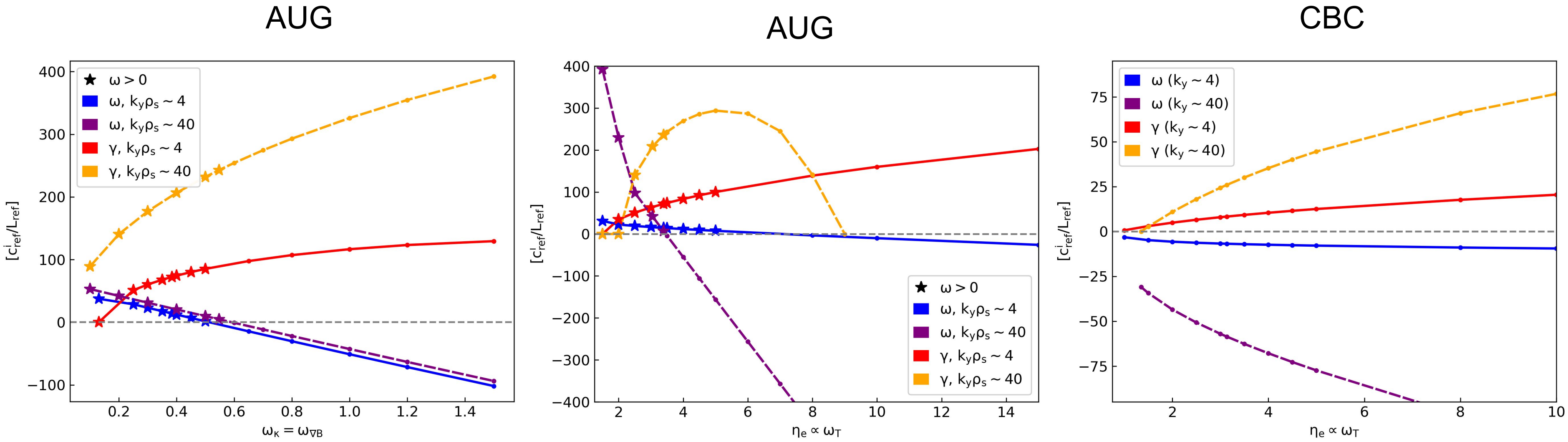

Backup slides - ion frequency ETG geometry scans

MxH coefficients

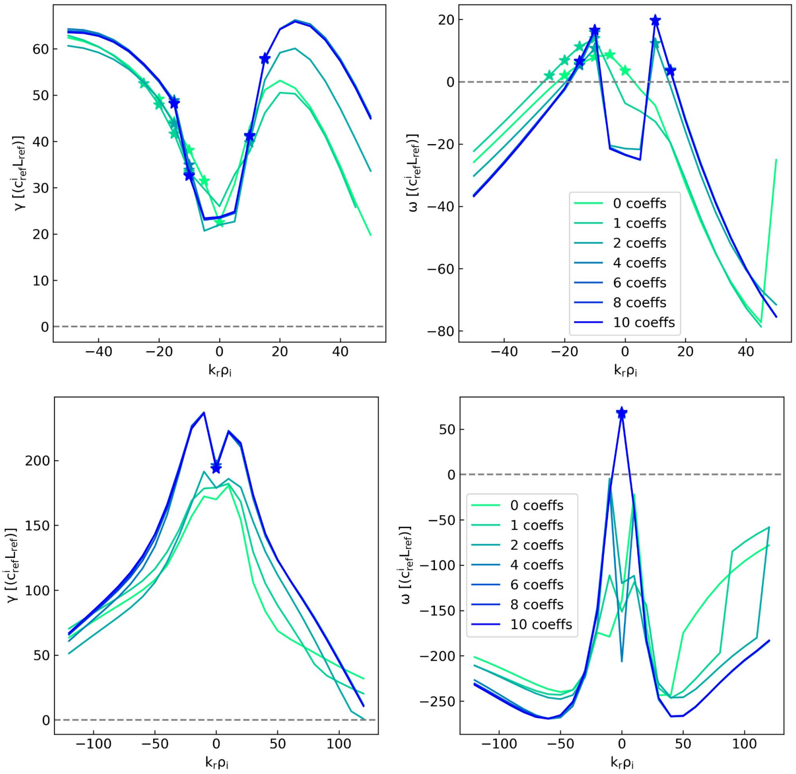

q scan

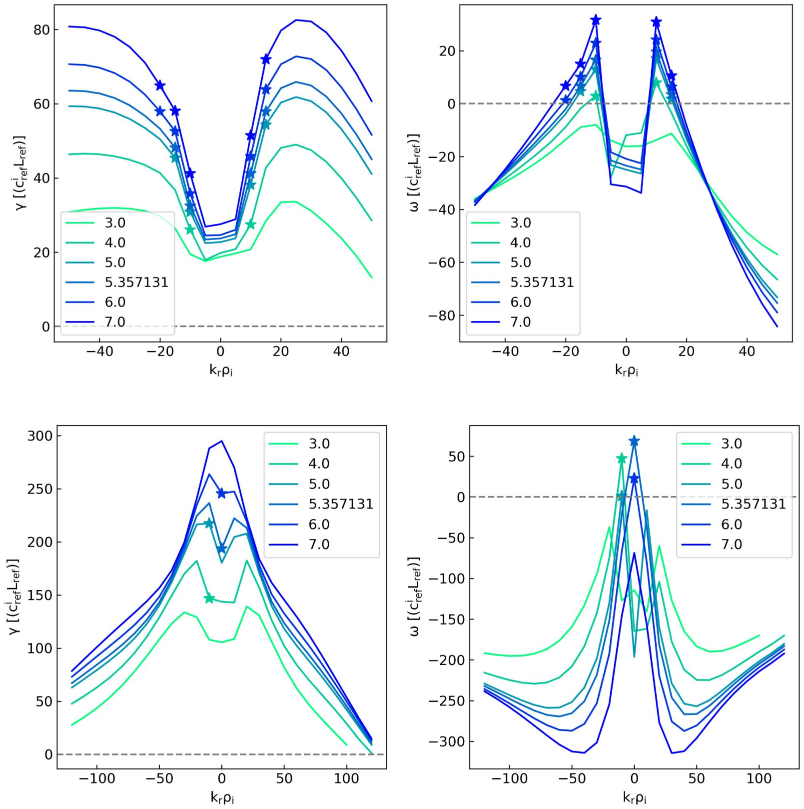

Backup slides - ion frequency ETG geometry scans

Kappa scan

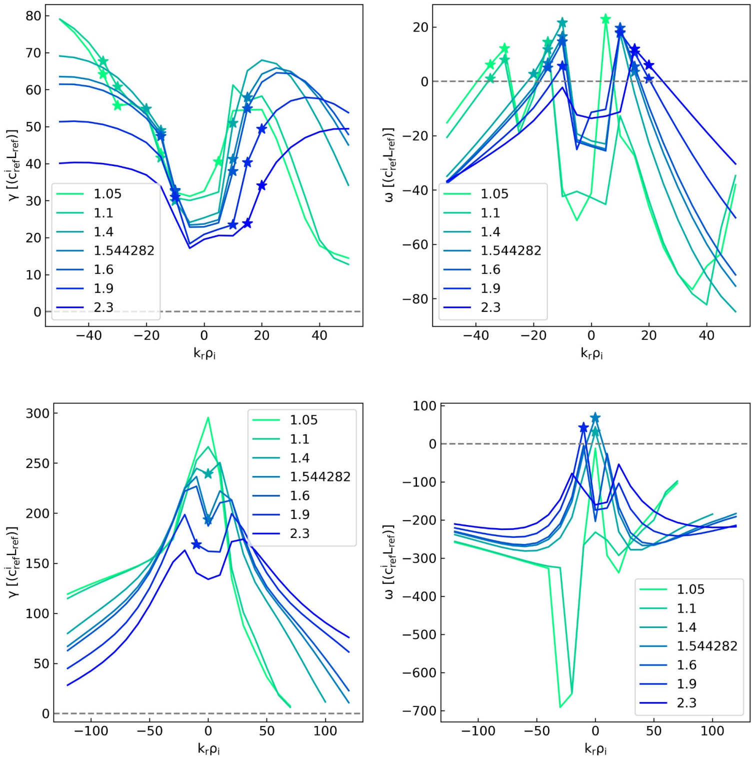

Magnetic shear scan

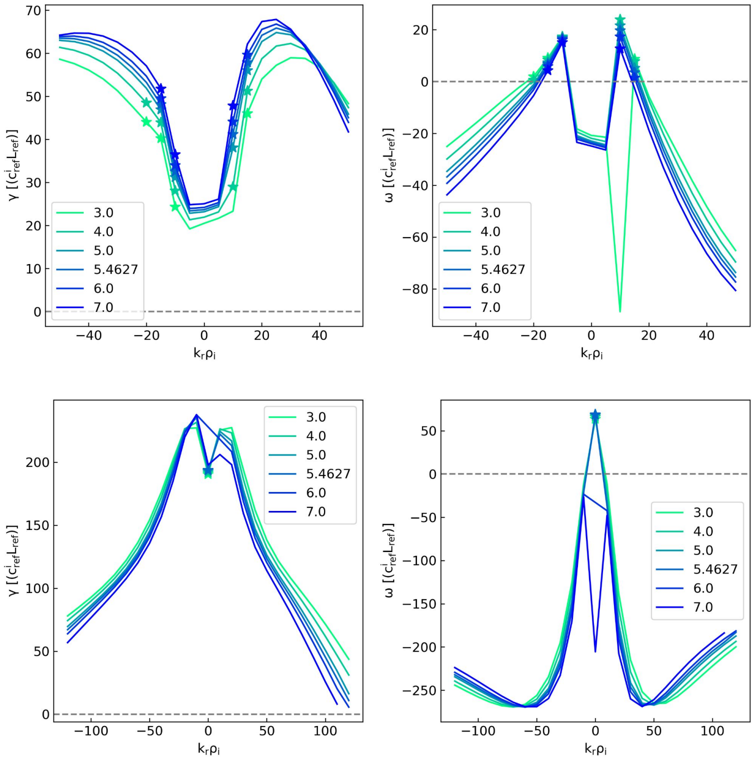

Backup slides - ion frequency ETG geometry scans

Kappa scan

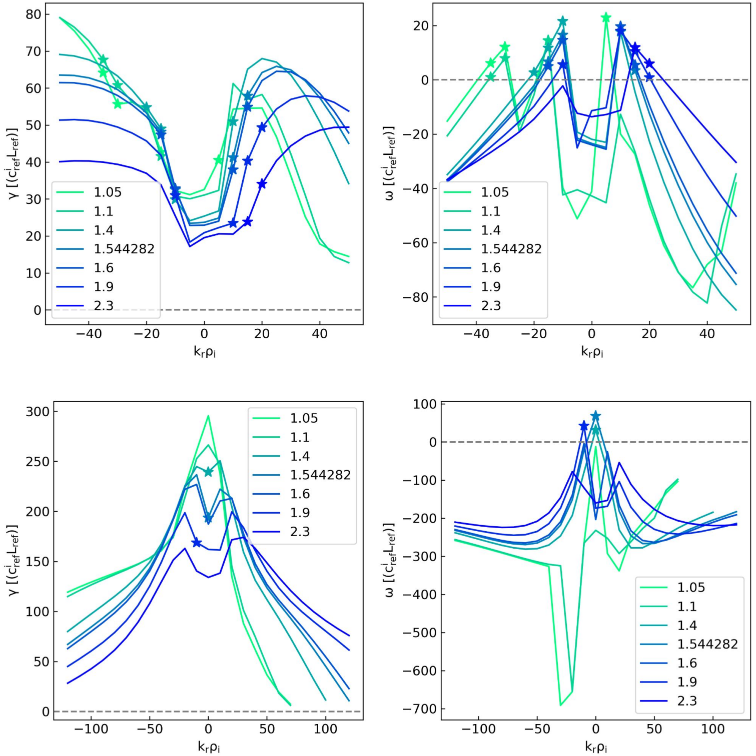

Magnetic shear scan

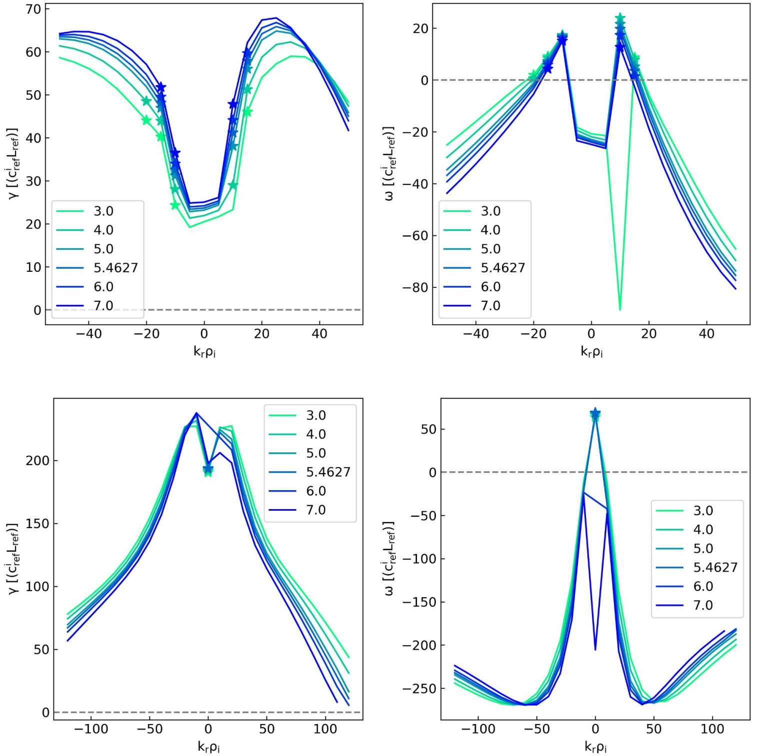

Local electron scale turbulence

- Impact of shaping is radially dependant.

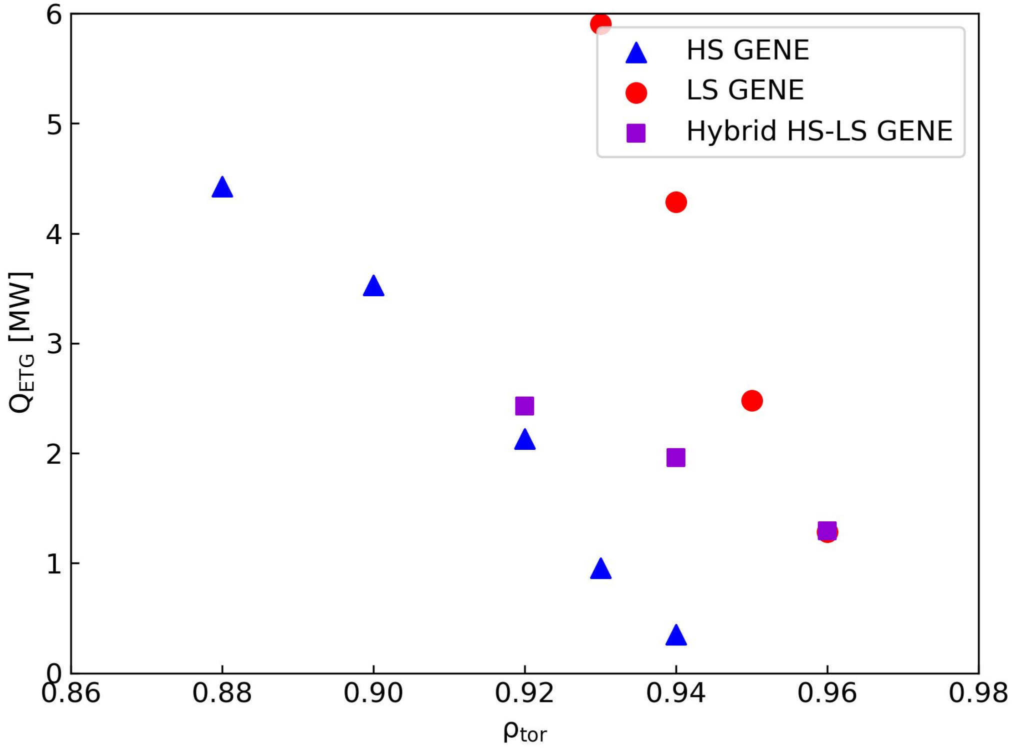

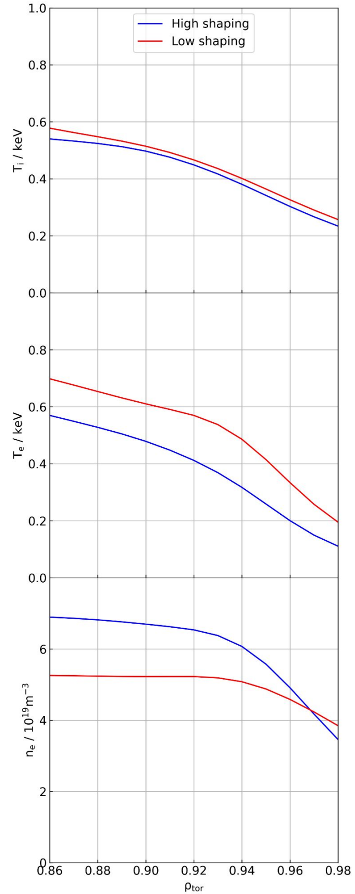

Grid size: $(n_s,n_x,n_{ky},n_z,n_v,n_w)$=(1,256+,48,512,32,16); Physics: e species, collisions, no ExB shear

Backup slides - nonlinear ETG

Hyp_z & nz0 scan for nonlinear ETG

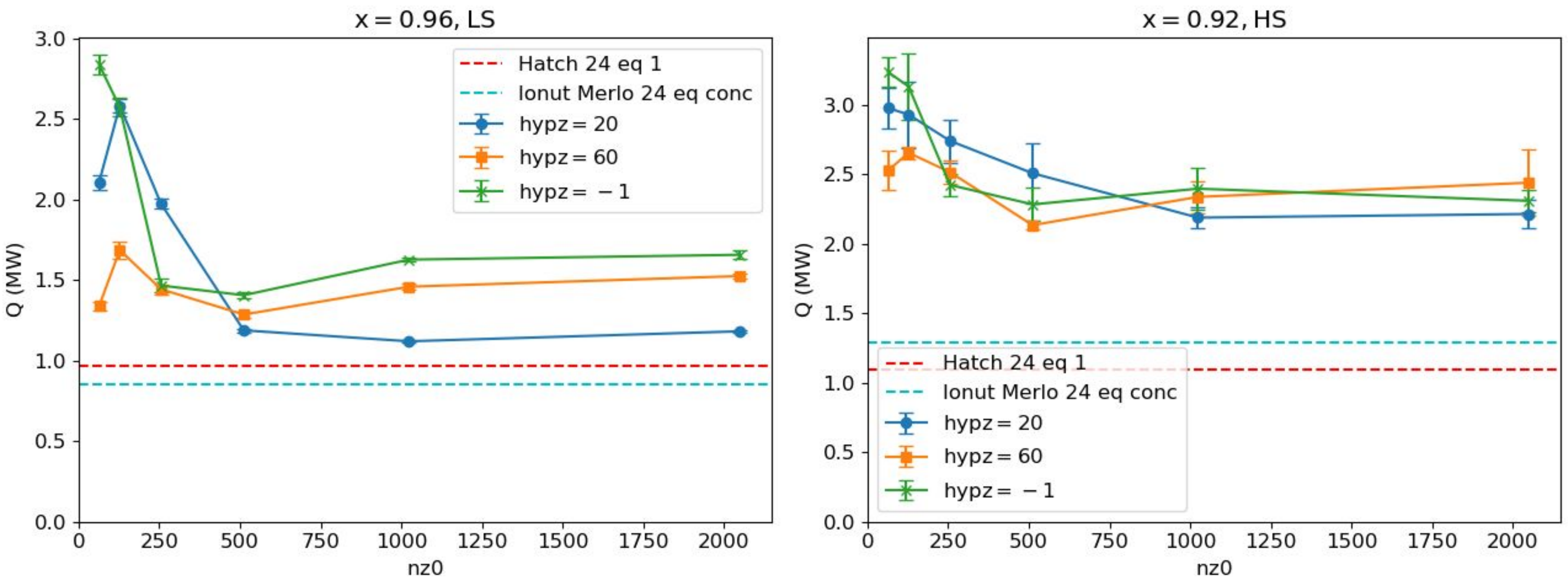

Additional information

$$\omega_{\kappa s} \equiv \frac{v_{ts}^2 \mathbf{k}_\perp}{\Omega_s} \cdot \left(\hat{\mathbf{b}} \times \left(\nabla \ln B + \frac{4\pi}{B^2} \frac{\partial p_0}{\partial r} \nabla r \right) \right)$$

$$\omega_{\nabla B s} \equiv \frac{v_{ts}^2 \mathbf{k}_\perp}{\Omega_s} \cdot (\hat{\mathbf{b}} \times \nabla \ln B).$$

$$\omega_{*s} \equiv -\frac{c}{B} \frac{T_{0\,s}}{Z_s e L_{ns}} (\mathbf{k}_\perp \times \hat{\mathbf{b}}) \cdot \nabla r = \frac{c}{B_a} \frac{T_{0\,s}}{Z_s e L_{ns}} k_y$$

Additional information

The gyrokinetic ordering:

$$\frac{f_1}{F_0} \sim \frac{q\phi_1}{T_e} \sim q\frac{v_\|}{c}\frac{A_{1\|}}{T_e} \sim \frac{B_{1\|}}{B} \sim \epsilon_\delta \qquad \frac{\rho_i \nabla F_0}{F_0} \sim \epsilon_F$$

$$\frac{\rho_i \nabla B}{B} \sim \epsilon_B$$

$$\frac{k_\|}{k_\perp} \sim \epsilon_\| \qquad \frac{\omega}{\Omega} \sim \epsilon_\omega$$

Why delta f works even at very high values?

n_1 is generally small due to the sources fixing the profiles.

Vlasov equation

$$\begin{aligned}\frac{\partial F_{1,\sigma}}{\partial t} = &- \left[v_\|\mathbf{b}_0 + (\mathbf{v}_\chi + \mathbf{v}_{\nabla B} + \mathbf{v}_c)\right] \cdot \nabla F_{1,\sigma} + \frac{\mu}{m_\sigma}\mathbf{b}_0 \cdot \nabla B_0 \frac{\partial F_{1,\sigma}}{\partial v_\|} \\ &- \mathbf{v}_\chi \cdot \left[\nabla \ln(n_{0,\sigma}) + \nabla \ln(T_{0,\sigma})\left(\frac{m_\sigma v_\|^2/2 + \mu B_0}{T_{0,\sigma}} - \frac{3}{2}\right)\right] F_{M,\sigma} \\ &- \frac{q_\sigma F_{M,\sigma}}{T_{0,\sigma}}\left[v_\|\mathbf{b}_0 + (\mathbf{v}_\chi + \mathbf{v}_{\nabla B} + \mathbf{v}_c)\right] \cdot \nabla \mathcal{G}\{\psi_1\} \\ &- \frac{q_\sigma v_\|}{c}\frac{F_{M,\sigma}}{T_{0,\sigma}}\frac{\partial \mathcal{G}\{A_{1,\|}\}}{\partial t} - \mathbf{v}_{E_0} \cdot \left(\nabla F_{1,\sigma} + \frac{q_\sigma v_\|}{c}\nabla \mathcal{G}\{A_{1,\|}\}\right) \\ &- (\mathbf{v}_{\nabla B} + \mathbf{v}_c) \cdot \left[\nabla \ln(n_{0,\sigma}) + \nabla \ln(T_{0,\sigma})\left(\frac{m_\sigma v_\|^2/2 + \mu B_0}{T_{0,\sigma}} - \frac{3}{2}\right)\right] F_{M,\sigma}.\end{aligned} \tag{2.7.3}$$

[F. Wilms, PhD thesis (2024)]